

Five-mode linear optical scheme for Bell state generation

Suren A. Fldzhyan, Mikhail Yu. Saygin,* and Sergei P. Kulik

*Quantum Technology Centre of Faculty of Physics,
M. V. Lomonosov Moscow State University, Moscow, Russian Federation*

The capability of linear optics to generate entangled states is widely exploited in quantum information processing, however, it is non-trivial to generate qubit states. Here we investigate the linear optical methods for generation of dual-rail-encoded Bell states using computer optimization. We have found a five-mode scheme that produces these states with probability $1/9$ with heralding by one photon detector. This result is an improvement in both compactness and success probability compared to the previously known schemes requiring six-mode transformations and two photon detectors and providing a success probability of $2/27$. We show that the increase in success probability is due to the elevated order of photon interference implemented by our scheme: four photons interfere in our scheme, while three photons interfere in the known scheme.

INTRODUCTION

Linear optics can generate non-classical states of light using initially separable single photons. The simplest example of entangled states produced by linear optics is the one produced by interference of two single photons on a balanced beam-splitter, constituting the well-known Hong-Ou-Mandel effect [1]. Similarly, large-scale entangled states can also be obtained by linear optics, as in the case of boson sampler, where multiple photons on a multimode interferometer [2, 3].

However, most often, performing quantum information tasks requires logical qubit encoding rather just superposition of photons. This necessity imposes severe constraints on the transformation capabilities of linear optical schemes making the generation of logical states non-deterministic [4], and logical operations over these states even more so [5, 6]. As a result of this, the generation of high-dimensional entangled qubit states directly by multimode linear optics is impractical.

For this reason, the current interest is focused on ways of generating small-scale resource states that can serve as building blocks of more complex states used in quantum communication [7, 8] and quantum computing [9, 10]. The maximally entangled dual-rail-encoded Bell states, which is the state of our interest in this work, are the easiest and most applicable entanglement resource [11]. Another example of a small-scale resource state is the three-photon Greenberger-Horne-Zeilinger [12] widely used in photonic measurement-based quantum computing [9, 13, 14].

Remarkably that solving seemingly simple tasks, even the development of schemes for generation of two- and three-qubit resource states, can be problematic for human intuition due to the extraordinary behaviour of photons at interference, thereby making the development unproductive or suboptimal [4, 15]. To aid in designing experiments, the quantum information of today is enjoying the proliferation of computer methods not long

ago utilized solely in the classical domain, which constituent methods of machine learning and artificial intelligence [4, 16–19].

It should be emphasized that one can categorize the quantum linear optical schemes according to the access to active feed-forward. In schemes with active feed-forward any generated state differing from the target Bell state by a permutation of modes is considered as success, since it can be transformed accordingly [20]. In contrast, static schemes are designed to generate one particular Bell state [4, 19]. Generally, using active schemes yields higher success probability of state generation, however, this comes with errors and losses introduced by the active elements into the quantum information algorithm. Of course, using one scheme or another in a large-scale photonic system is a matter of trade-offs. In this work, we use computer optimization to construct static linear optical schemes generating dual-rail-encoded Bell states out of single photons with the aim to find as compact and efficient scheme as possible.

From previous works it is known that four single photons at minimum are necessary to generate the dual-rail-encoded Bell states by linear optics [4, 19]. Also, at minimum six-mode interferometers that transform initially separable photons and two photon detectors were considered to produce the state [4, 19]. We improved the known schemes in both compactness and success probability, namely, a five-mode scheme requiring one auxiliary mode and one photon detector has been found.

The paper is organized as follows. In Sec. I we introduce linear optical schemes, which we consider to generate Bell states. In Sec. II, we describe the optimization procedure utilized to find optimal parameters of the schemes. The obtained results are given in Sec. III. We summarize in Sec. IV.

I. SCHEMES FOR BELL STATE GENERATION

There are four maximally entangled Bell states: $|\Psi^{(\pm)}\rangle = (|01\rangle_L \pm |10\rangle_L)/\sqrt{2}$, $|\Phi^{(\pm)}\rangle = (|00\rangle_L \pm |11\rangle_L)/\sqrt{2}$, where $|0\rangle_L$ and $|1\rangle_L$ are the logic basis states

* saygin@physics.msu.ru

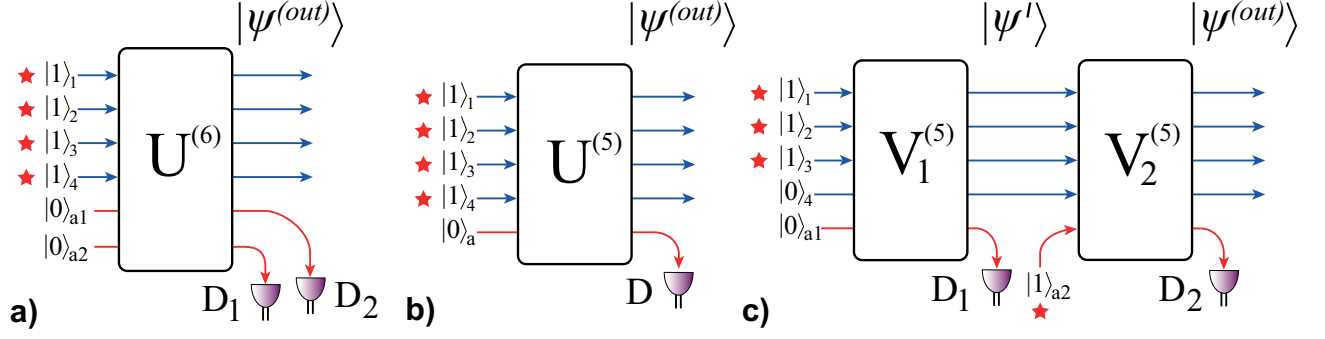


FIG. 1. Three types of linear optical schemes for generation of the dual-rail-encoded Bell states out of four separable photons: a) the scheme that use a six-mode interferometer $U^{(6)}$ and two photon detectors, D_1 and D_2 . For heralding both detectors should measure single photons. This type of scheme has been studied previously in [4]; b) the scheme that use a five-mode interferometer $U^{(5)}$ and one photon detector D . For heralding the detector should measures two photons; c) the scheme that uses a sequence of two five-mode interferometers two detectors, D_1 and D_2 . For heralding both detectors should measure single photons. In these schemes four modes are reserved for the Bell state.

of a qubit. State $|\Psi^{(\pm)}\rangle$, $|\Phi^{(\pm)}\rangle$ are connected with each other by local operations so that any of the states can be obtained from another by applying single-qubit operator. For example, assuming state $|\Phi^{(+)}\rangle$ at hand, the other states are derived by: $|\Phi^{(-)}\rangle = \hat{Z}_1|\Phi^{(+)}\rangle$, $|\Psi^{(+)}\rangle = \hat{X}_1|\Phi^{(+)}\rangle$, and $|\Psi^{(-)}\rangle = \hat{X}_1\hat{Z}_1|\Phi^{(+)}\rangle$, where \hat{X}_j and \hat{Z}_j are the Pauli operators with the subscript j referring to a mode the operator is applied to.

Here, we consider the dual-rail encoding method that require two spatial modes and one photon per one qubit, so that an arbitrary one-qubit state is a superposition over the physical Fock states: $|0\rangle_L = |1\rangle_1|0\rangle_2$ and $|1\rangle_L = |0\rangle_1|1\rangle_2$, where $|0\rangle_j$ and $|1\rangle_j$ are states with 0 and 1 photon in mode j , respectively. The encoding method is conveniently implemented, for example, by integrated photonics platform, enabling creation of large-scale quantum devices. Also, arbitrary single-qubit operations are implemented easily and deterministically by the programmable two-port Mach-Zehnder interferometers. Therefore, dual-rail encoding is the choice in many realizations of quantum information processing tasks [5]. Without loss of generality, as a concrete example we are interested in the generation of the Bell state $|\Phi^{(+)}\rangle$ having the following physical state:

$$|\Phi\rangle = \frac{1}{\sqrt{2}}(|1010\rangle + |0101\rangle), \quad (1)$$

where the superscript will be omitted in the following.

By contrast, in the dual-rail encoding entangling two-qubit operations are probabilistic and require extra resources of photons and modes of transformations, in addition to those reserved for qubit encoding itself. In particular, it is known that the linear optical generation of the Bell states requires at least four photons, two of which are to be measured in the auxiliary modes of the optical scheme, wherein a suitable sequence of the detection events will unambiguously herald the target state leaving the scheme [4, 19]. We are attempting to improve

the generation process of the Bell states to achieve a higher success probability, while using minimum spatial resources.

Fig. 1 illustrates three optical schemes considered as means to generate a Bell state. The first scheme depicted in Fig. 1a exploits a six-mode linear optical interferometer $U^{(6)}$ that make four initially separable input photons interfere with each other. It is known from prior works [4, 19] that the Bell states may be produced in this kind of six-mode schemes when the transfer matrix of the interferometer is properly chosen and two photon detectors, D_1 and D_2 , are using for heralding that should measure photons, one per detector. It has been found that the probability with which the detection event takes place was found to be $2/27$. We use this type of scheme as a well-known example to compare the results of other two types of schemes and to assess the correctness of the optimization algorithm described in the section that follows.

The second scheme, which is depicted in Fig. 1b, to the best of our knowledge, has not been considered before. It exploits a five-mode interferometer $U^{(5)}$ and one photon detector D , which makes it more compact than the first one. Because of one auxiliary mode, two photons can be removed by measuring them by the detector. Our goal is to prove that interferometer $U^{(5)}$ does exist that guarantee generation of the Bell state, find its optimal form characterized by as minimal number of elements as possible and highest success probability.

Also, we introduce the third scheme shown in Fig. 1c, in order to study the effect of the order of photon interference on the capability to generate Bell states. This scheme exploits a sequence of two interferometers, $V_1^{(5)}$ and $V_2^{(5)}$ and photodetection at after each of them. Three photons enter the first interferometer that produces an intermediate state $|\psi'\rangle$, that partly measured by detector D_1 . If one photon is measured, then the procedure proceeds by sending the unmeasured part of the inter-

mediate state to the second interferometer together with one fresh photon. In the end, measuring one photon by the second detector D_2 heralds the Bell state leaving the scheme. By construction, the scheme purposefully limits the number of photons that can interact in interferometers to three. Notice that in the first two schemes four photons are allowed to interfere simultaneously.

II. OPTIMIZATION PROCEDURE

The state at the output of a lossless N -mode interferometer is the superposition over multiple basis states:

$$|\psi\rangle_{sa} = \sum_{\mathbf{t}} c_{\mathbf{t},\mathbf{s}} |\mathbf{t}\rangle_{sa}, \quad (2)$$

where vectors $\mathbf{s} = (s_1, \dots, s_N)$ and $\mathbf{t} = (t_1, \dots, t_N)$ denote the photon occupation vectors of the input and output, respectively. In general, the sum in (2) runs through all possible vectors \mathbf{t} , which number grows as $\binom{M+N-1}{M}$, where M is the number of photons and N is the number of modes. As the total number of photons is conserved by the lossless transformation, it follows that $\sum_j s_j = \sum_j t_j = M$. Following the assignment of modes adopted in Fig. 2, the basis states are split into the logical (s) and auxiliary (a) part: $\mathbf{t} = \mathbf{t}_s \oplus \mathbf{t}_a$, so that $|\mathbf{t}\rangle_{sa} = |\mathbf{t}_s\rangle_s |\mathbf{t}_a\rangle_a$. The probability amplitudes are calculated by $c_{\mathbf{t},\mathbf{s}} = \text{perm}(U_{\mathbf{t},\mathbf{s}}) / \sqrt{\mathbf{t}! \cdot \mathbf{s}!}$, where $\text{perm}(U_{\mathbf{t},\mathbf{s}})$ is the permanent of matrix $U_{\mathbf{t},\mathbf{s}}$, which is obtained by taking the columns and rows of the transfer matrix of the interferometer U according to vectors \mathbf{s} and \mathbf{t} , respectively [21]; $\mathbf{s} = s_1! \dots s_N!$ and $\mathbf{t} = t_1! \dots t_N!$ is the shorthand for factorials.

To parametrize the transfer matrices of the interferometers constituent the schemes depicted in Fig. 1, we use the universal decomposition of unitary matrices suggested in [22]. The decomposition represents an N -mode interferometer as N layers consisting of beam-splitters with variable transmissivities and variable phase shifts. Each beam-splitter act locally on two neighboring modes by the transfer matrix:

$$T_j(\theta, \varphi) = \begin{pmatrix} e^{i\varphi} \sin \theta & \cos \theta \\ e^{i\varphi} \cos \theta & -\sin \theta \end{pmatrix}, \quad (3)$$

where θ specifies the transmissivity of the beam-splitter $\tau = \cos^2 \theta$ ($0 \leq \theta \leq \pi/2$), φ is the phase difference between the input modes of the beam-splitter ($-\pi \leq \varphi < \pi$). The resultant multimode transfer matrix is the product of $Q = N(N-1)/2$ matrices: $U = D \cdot T_Q^{(n_Q, m_Q)} \dots T_1^{(n_1, m_1)}$, with D being a diagonal matrix of independent phase shifts α_i ($i = \overline{1, N-1}$) and $T_q^{(m_q, n_q)}$ is the beam-splitter matrix acting on modes m_q and n_q . It has been proven that this way an arbitrary $N \times N$ transfer matrix can be parametrized by proper setting the phase shifts [22].

Non-deterministic schemes generate the demanded quantum states heralded by a pattern of photons \mathbf{d} detected in the auxiliary modes with a success probability p . Thus, it follows that the output quantum state has the form:

$$|\Psi_0\rangle_{sa} = \sqrt{p} |\Phi\rangle_s |\mathbf{d}\rangle_a + \sqrt{1-p} |R\rangle_{sa}, \quad (4)$$

where $|R\rangle_{sa}$ is the byproduct component of the state always present in non-deterministic linear optical schemes. Of course, for practical reasons, the interferometers should provide maximum success probability p . However, even small admixture of a component that contradict the dual-rail encoding degrades the quality of the target state. For example, it can introduce errors in the algorithm the state is used for or make its usage impossible altogether. Hence, the necessary requirement is that the term $|R\rangle_{sa}$ should not contain amplitudes at basis states, whose auxiliary part coincide with $|\mathbf{d}\rangle$, used for heralding success.

Also notice that in (3), values $\theta = 0$ and $\theta = \pi/2$ correspond to the trivial crossover and identity transformations, which are more easy to implement in practice than a general two-mode beam-splitter with a specific splitting ratio. Therefore, in addition to the necessary requirements, we also demand that the interferometers are constructed from minimal number of elements.

To find optimal decomposition of interferometer, we use optimization algorithm that explore the parameter space of the linear optical circuits to find the global maximum of a cost function that account for the aforementioned requirements. Specifically, we used the L-BFGS algorithm, which home-made code has been implemented in C++ [23].

In optimization, the algorithm was exploring the space of phase-shifts that parametrize the interferometer(-s) to minimize the following cost function:

$$f(\vec{\theta}, \vec{\varphi}) = -\tilde{p}^\mu F + \varepsilon \sum_{j=1}^Q (\sin^2 2\theta_j + \sin^2 2\varphi_j), \quad (5)$$

with \tilde{p} being the probability of obtaining state with $|\mathbf{d}\rangle_a$ in the auxiliary modes calculated by $\tilde{p} = \langle \chi_{\mathbf{d}} | \chi_{\mathbf{d}} \rangle$, where $|\chi_{\mathbf{d}}\rangle = {}_a \langle \mathbf{d} | \Psi^{(out)} \rangle_{sa}$ is the unnormalized state of the logical modes, $F = |\langle \chi_{\mathbf{d}} | \Phi \rangle|^2 / \tilde{p}$ is fidelity. Taking the form of the state (4) into account, F attain its maximum value of 1 if and only if $|\chi_{\mathbf{d}}\rangle = |\Phi\rangle$. The second term in (5) penalizes the occurrence of non-trivial beam-splitters and phase-shifts in the decomposition. Parameters μ and ε control the interplay between the two terms in (5) and their values are chosen for better convergence of the algorithm.

III. RESULTS

To avoid falling the algorithm into a local minimum and to guarantee convergence of the loss function into

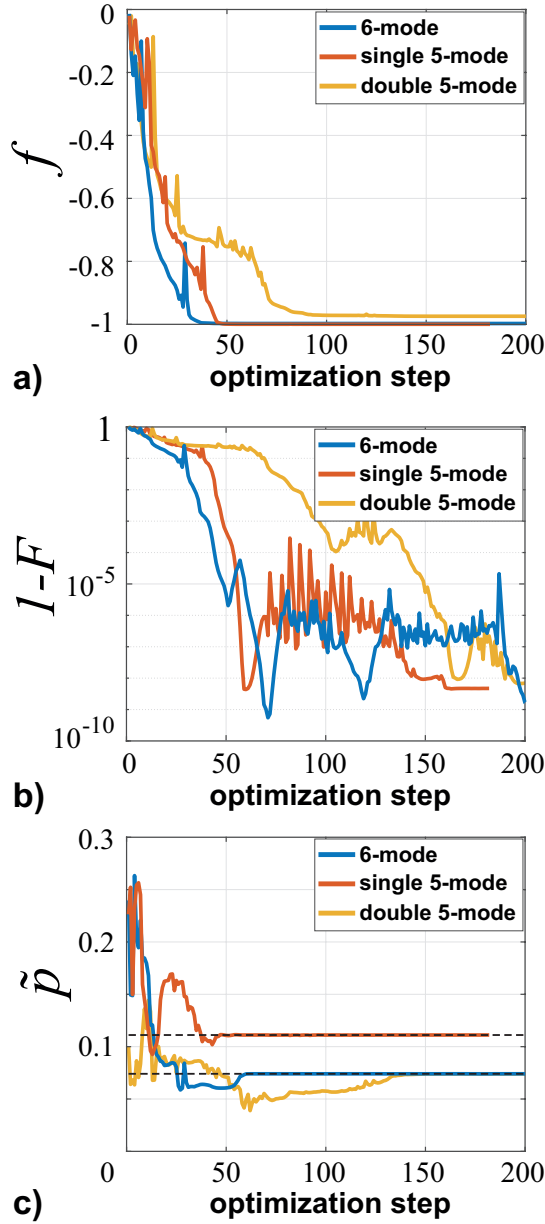


FIG. 2. The illustration of the optimization procedure: a) the cost function f depending on optimization step, b) the state infidelity $1 - F$ and c) probability \tilde{p} in the course of the optimization. The dashed lines mark probability levels of $2/27$ and $1/9$. The following parameters were used in the optimization algorithm: $\mu = 10^{-3}$, $\mu = 10^{-4}$, $\mu = 10^{-2}$ for the three schemes under study in order they are present in Fig. 1; $\varepsilon = 10^{-5}$ for all three schemes.

the global minimum, it was run several times (typically $\sim 3 - 5$), each time initializing the phase-shifts with random values. Fig. 2 gives examples of converging runs used to find the layouts of the interferometers. The dependencies of the cost function (5), which was the optimized function, is shown in Fig. 2a. The dependencies of the state infidelity $1 - F$ and probability \tilde{p} that accompany the optimized cost function are shown in Fig. 2b

and Fig. 2c, respectively.

Firstly, we found the layout of the six-mode interferometer $U^{(6)}$ (see Fig. 1a), shown in Fig. 3. It is constructed from two beam-splitters with $\tau = 2/3$ and three balanced beam-splitters with $\tau = 1/2$. The following state is generated by the interferometer:

$$|\psi^{(out)}\rangle = \sqrt{\frac{2}{27}}|\Phi\rangle_s|1\rangle_{a1}|1\rangle_{a2} + \frac{5}{\sqrt{27}}|R^{(6)}\rangle_{sa}. \quad (6)$$

Due to cumbersomeness, the explicit form of the residual term $|R^{(6)}\rangle_{sa}$ is given in the Supplementary section (the same is true for the residual terms corresponding to the rest of the schemes). From (6) it follows that the Bell state $|\Phi\rangle_s$ is generated with probability $p = 2/27$ conditioned upon detection of two single photons by detectors D_1 and D_2 . This result is in agreement with the result of [4], however, the difference is in one extra beam-splitter required by the interferometer from [4] and different placement of the elements. Therefore, we infer that our six-mode scheme is less complex to implement.

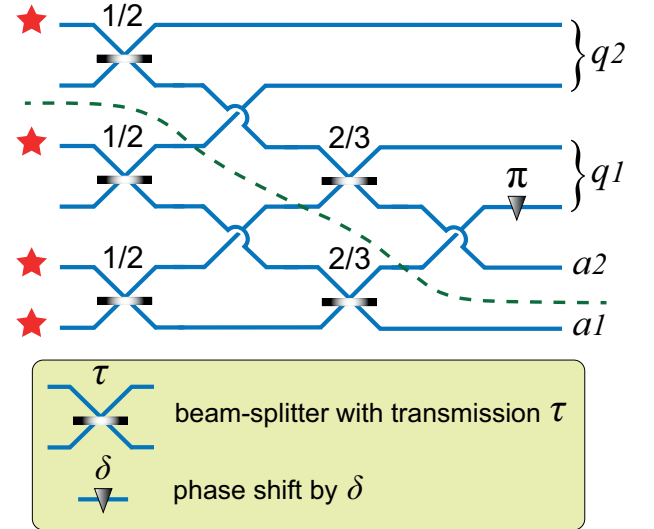


FIG. 3. The explicit six-mode scheme obtained by optimization. Here, q_1 and q_2 are the pairs of modes that encode logical qubits, a_1 and a_2 are auxiliary modes to be measured by the detectors (see Fig. 1a). The beam-splitters are marked by their power transmissivities τ_j . The dashed line separates the scheme into two parts, in each of which three-photon interference take place, provided that one photon is measured in mode a_1 .

Interestingly, the layout of the six-mode interferometer suggests that four photons never interfere simultaneously with each other in case when the heralding detection events takes place. To demonstrate this, the dashed line drawn in the layout separates it into two parts. Obviously, one photon entering the upper part is not allowed to get into the lower part. The rest three photons interfere in the lower part and one of them is removed from it in the event of heralding performed on mode a_1 . This in turn guarantees that a two-photon state goes into the upper part where it interacts with the single-photon state,

producing a three-photon state at the output of the logical modes and mode a2.

The five-mode interferometer $U^{(5)}$ found by optimization is shown in Fig. 4. The output state it produces has the following form:

$$|\psi^{(out)}\rangle = \frac{1}{3}|\Phi\rangle_s|2\rangle_a + \frac{2\sqrt{2}}{3}|R^{(5,2)}\rangle_{sa}, \quad (7)$$

where the first term contains the Bell state (1) heralded by the presence of 2 photons in the auxiliary mode. The scheme generates the Bell state with probability 1/9, which is a significant improvement over the previous result. Remarkably, the scheme is built with the same number of beam-splitters and phase-shifts as the six-mode one. It is important to note that, unlike the six-mode scheme, the five-mode scheme exhibits four-photon interference, as one cannot divide the layout the way we do above. Also, this fact can be proved by the explicit form of the residual term $|R^{(5,2)}\rangle_{sa}$ given by (12), which has probability amplitudes corresponding to all four photons "focused" in one mode.

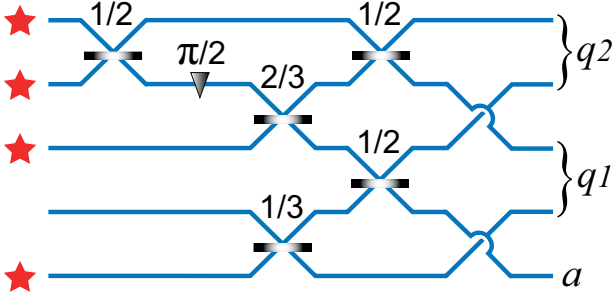


FIG. 4. The explicit five-mode scheme obtained by optimization (see Fig. 1b). The interferometer provides Bell state generation with probability of 1/9 heralded by detection of 2 photons in the auxiliary mode a. The designations are the same as in Fig. 3.

The interferometers $V_1^{(5)}$ and $V_2^{(5)}$ of the scheme depicted in Fig. 1c are shown in Fig. 5. In the first interferometer three initially separable photons interfere to produce the intermediate state $|\psi'\rangle$.

$$|\psi'\rangle = \frac{\sqrt{5}}{3}|\chi'_0\rangle_s|0\rangle_{a1} + \frac{1}{3}\sqrt{\frac{5}{2}}|\chi'_1\rangle_s|1\rangle_{a1} + \frac{1}{3}|\chi'_2\rangle_s|2\rangle_{a1} + \frac{1}{3\sqrt{2}}|0000\rangle_s|3\rangle_{a1}, \quad (8)$$

where states $|\chi'_j\rangle_s$ are given explicitly in the Supplemental section (see (15)). The auxiliary mode a1 is measured by photon detector and at single photon event, the generation proceeds by directing the state $|\chi_1\rangle_s$ into the second

interferometer together with extra photon that goes into the auxiliary mode a2. Then, the state at the output of the second interferometer has the following form:

$$|\psi^{(out)}\rangle = \frac{2}{\sqrt{15}}|\Phi\rangle_s|1\rangle_{a2} + \sqrt{\frac{11}{15}}|R^{(5,1,1)}\rangle_{sa2}. \quad (9)$$

As the generation success is conditioned by the events of single photons being detected by D_1 and D_2 . From (8) and (9) it follows that the probability of measuring one photon by D_1 and D_2 is 5/18 and 4/15, respectively. Accordingly, the overall probability to generate the Bell state is the product of these values, which yields 2/27. Therefore, this once again prove that the difference in success probabilities with which linear optical schemes generate the Bell state is connected with the order of photon interference.

IV. CONCLUSION

In this work, we investigated the linear optical generation of the dual-rail-encoded Bell states. Using a computer optimization algorithm, we have improved the six-mode schemes, which were previously considered as the most compact ones, in both compactness and the success probability. Namely, the five-mode scheme that require one photodetector has been found. Besides being the most compact, our scheme also offers a much higher generation probability of 1/9 than in the previous schemes, for which the generation probability was 2/27. Along the way, we have shown that the increase in success probability is connected with the elevated order of photon interference implemented by our scheme: four photons interfere in our scheme, while three photons interfere in the known schemes. These findings highlight the importance of computer methods in designing quantum optical setups, which will be playing more integral role in the development process of practical quantum devices in the future.

V. ACKNOWLEDGMENTS

S.A. Fldzhyan and M.Yu. Saygin are grateful for support the Foundation for the Advancement of Theoretical Physics and Mathematics (BASIS) (grants № 20-2-1-97-1 and № 20-1-3-31-1). The authors acknowledge partial support by the Interdisciplinary Scientific and Educational School of Moscow University "Photonic and Quantum Technologies. Digital Medicine".

[1] C. K. Hong, Z. Y. Ou, and L. Mandel, Measurement of subpicosecond time intervals between two photons by in-

terference, *Phys. Rev. Lett.* **59**, 2044 (1987).

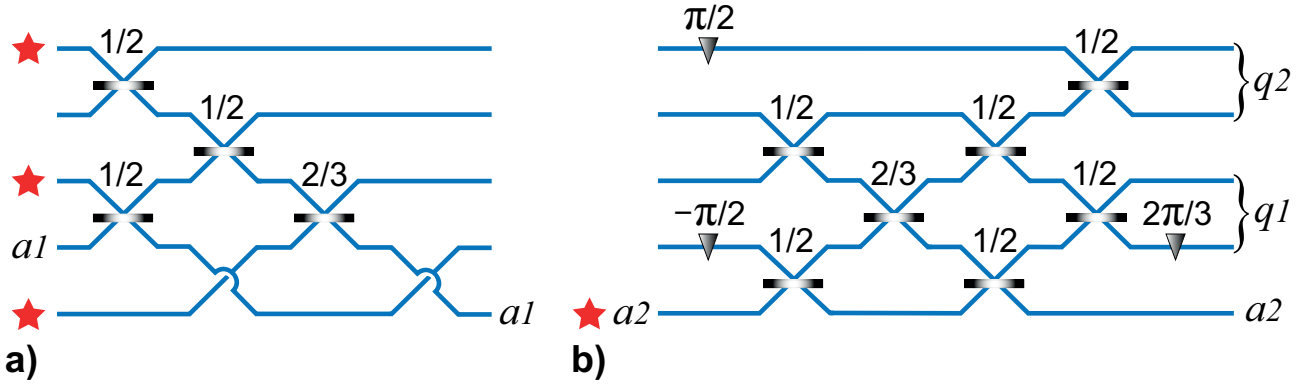


FIG. 5. The five-mode interferometers, $V_1^{(5)}$ (a) and $V_2^{(5)}$ (b), constituent the scheme depicted in Fig. 1c, which were obtained by optimization. The designations are the same as in Fig. 3.

- [2] H. Wang, J. Qin, X. Ding, M.-C. Chen, S. Chen, X. You, Y.-M. He, X. Jiang, L. You, Z. Wang, C. Schneider, J. J. Renema, S. Höfling, C.-Y. Lu, and J.-W. Pan, Boson sampling with 20 input photons and a 60-mode interferometer in a 10^{14} -dimensional hilbert space, *Phys. Rev. Lett.* **123**, 250503 (2019).
- [3] H.-S. Zhong, H. Wang, Y.-H. Deng, M.-C. Chen, L.-C. Peng, Y.-H. Luo, J. Qin, D. Wu, X. Ding, Y. Hu, P. Hu, X.-Y. Yang, W.-J. Zhang, H. Li, Y. Li, X. Jiang, L. Gan, G. Yang, L. You, Z. Wang, L. Li, N.-L. Liu, C.-Y. Lu, and J.-W. Pan, Quantum computational advantage using photons, *Science* **370**, 1460 (2020).
- [4] F. V. Gubarev, I. V. Dyakonov, M. Y. Saygin, G. I. Struchalin, S. S. Straupe, and S. P. Kulik, Improved heralded schemes to generate entangled states from single photons, *Phys. Rev. A* **102**, 012604 (2020).
- [5] J. Carolan, C. Harrold, C. Sparrow, E. Martín-López, N. J. Russell, J. W. Silverstone, P. J. Shadbolt, N. Matsuda, M. Oguma, M. Itoh, G. D. Marshall, M. G. Thompson, J. C. F. Matthews, T. Hashimoto, J. L. O’Brien, and A. Laing, Universal linear optics, *Science* **349**, 711 (2015).
- [6] D. B. Uskov, L. Kaplan, A. M. Smith, S. D. Huver, and J. P. Dowling, Maximal success probabilities of linear-optical quantum gates, *Phys. Rev. A* **79**, 042326 (2009).
- [7] J. Wallnöfer and W. Dür, Measurement-based quantum communication with resource states generated by entanglement purification, *Phys. Rev. A* **95**, 012303 (2017).
- [8] P. Hilaire, E. Barnes, S. E. Economou, and F. Grosshans, Error-correcting entanglement swapping using a practical logical photon encoding (2021), [arXiv:2101.11082 \[quant-ph\]](https://arxiv.org/abs/2101.11082).
- [9] M. Gimeno-Segovia, P. Shadbolt, D. E. Browne, and T. Rudolph, From three-photon greenberger-horne-zeilinger states to ballistic universal quantum computation, *Phys. Rev. Lett.* **115**, 020502 (2015).
- [10] Y. Li, P. C. Humphreys, G. J. Mendoza, and S. C. Benjamin, Resource costs for fault-tolerant linear optical quantum computing, *Phys. Rev. X* **5**, 041007 (2015).
- [11] M. A. Nielsen and I. L. Chuang, *Quantum Computation and Quantum Information: 10th Anniversary Edition* (Cambridge University Press, 2010).
- [12] W. Dür, G. Vidal, and J. I. Cirac, Three qubits can be entangled in two inequivalent ways, *Phys. Rev. A* **62**, 062314 (2000).
- [13] S. Bartolucci, P. Birchall, H. Bombin, H. Cable, C. Dawson, M. Gimeno-Segovia, E. Johnston, K. Kieling, N. Nickerson, M. Pant, F. Pastawski, T. Rudolph, and C. Sparrow, Fusion-based quantum computation (2021), [arXiv:2101.09310 \[quant-ph\]](https://arxiv.org/abs/2101.09310).
- [14] H. Bombin, I. H. Kim, D. Litinski, N. Nickerson, M. Pant, F. Pastawski, S. Roberts, and T. Rudolph, Interleaving: Modular architectures for fault-tolerant photonic quantum computing (2021), [arXiv:2103.08612 \[quant-ph\]](https://arxiv.org/abs/2103.08612).
- [15] M. Krenn, M. Erhard, and A. Zeilinger, Computer-inspired quantum experiments, *Nature Reviews Physics* **2**, 649 (2020).
- [16] M. Krenn, M. Malik, R. Fickler, R. Lapkiewicz, and A. Zeilinger, Automated search for new quantum experiments, *Phys. Rev. Lett.* **116**, 090405 (2016).
- [17] A. A. Melnikov, H. Poulsen Nautrup, M. Krenn, V. Dunjko, M. Tiersch, A. Zeilinger, and H. J. Briegel, Active learning machine learns to create new quantum experiments, *Proceedings of the National Academy of Sciences* **115**, 1221 (2018).
- [18] M. Erhard, M. Malik, M. Krenn, and A. Zeilinger, Experimental greenberger-horne-zeilinger entanglement beyond qubits, *Nature Photonics* **12**, 759 (2018).
- [19] S. Stanisic, N. Linden, A. Montanaro, and P. S. Turner, Generating entanglement with linear optics, *Phys. Rev. A* **96**, 043861 (2017).
- [20] Q. Zhang, X.-H. Bao, C.-Y. Lu, X.-Q. Zhou, T. Yang, T. Rudolph, and J.-W. Pan, Demonstration of a scheme for the generation of “event-ready” entangled photon pairs from a single-photon source, *Phys. Rev. A* **77**, 062316 (2008).
- [21] M. C. Tichy, Sampling of partially distinguishable bosons and the relation to the multidimensional permanent, *Phys. Rev. A* **91**, 022316 (2015).
- [22] W. R. Clements, P. C. Humphreys, B. J. Metcalf, W. S. Kolthammer, and I. A. Walmsley, Optimal design for universal multiport interferometers, *Optica* **3**, 1460 (2016).
- [23] R. H. Byrd, P. Lu, J. Nocedal, and C. Zhu, A limited memory algorithm for bound constrained optimization, *SIAM Journal on Scientific Computing* **16**, 1190 (1995).

SUPPLEMENTAL MATERIAL

Here are the explicit residual terms of the quantum states produced by the schemes, depicted in Fig. 1 with interferometers circuits shown in Fig. 3-5.

The residual term of the output state (6) produced by the six-mode scheme (see Fig. 3) has the form:

$$\begin{aligned}
 |R^{(6)}\rangle_{sa} = & \frac{2\sqrt{2}}{5}|\chi_{00}\rangle_s|00\rangle_a + \frac{2}{5}|\chi_{10}\rangle_s|10\rangle_a + \\
 & + \frac{2}{5}|\chi_{01}\rangle_s|01\rangle_a + \frac{\sqrt{2}}{5}|\chi_{20}\rangle_s|20\rangle_a + \\
 & + \frac{\sqrt{2}}{5}|\chi_{02}\rangle_s|02\rangle_a + \frac{1}{5}|\chi_{12}\rangle_s|12\rangle_a + \\
 & + \frac{1}{5}|\chi_{21}\rangle_s|21\rangle_a + \frac{1}{5}|\chi_{30}\rangle_s|30\rangle_a + \frac{1}{5}|\chi_{03}\rangle_s|03\rangle_a + \\
 & + \frac{1}{5\sqrt{2}}|0000\rangle_s|13\rangle_a - \frac{1}{5\sqrt{2}}|0000\rangle_s|31\rangle_a,
 \end{aligned} \tag{10}$$

where the states of the logical modes $|\chi_{ij}\rangle_s$ read

$$\begin{aligned}
 |\chi_{00}\rangle_s &= \frac{\sqrt{3}(|1102\rangle_s - |1120\rangle_s - |1003\rangle_s - |0130\rangle_s)}{4} + \\
 &+ \frac{(|1021\rangle_s + |0112\rangle_s + |0031\rangle_s - |0013\rangle_s)}{4}, \\
 |\chi_{01}\rangle_s &= \frac{\sqrt{3}(|1101\rangle_s + |0111\rangle_s)}{2\sqrt{2}} - \frac{|1020\rangle_s + |0030\rangle_s}{2}, \\
 |\chi_{10}\rangle_s &= \frac{\sqrt{3}(|1110\rangle_s - |1011\rangle_s)}{2\sqrt{2}} + \frac{|0102\rangle_s - |0003\rangle_s}{2}, \\
 |\chi_{02}\rangle_s &= \frac{\sqrt{3}(|1100\rangle_s + |0011\rangle_s)}{4} + \frac{|0110\rangle_s + 3|1001\rangle_s}{4}, \\
 |\chi_{20}\rangle_s &= \frac{|1001\rangle_s + 3|0110\rangle_s}{4} - \frac{\sqrt{3}(|1100\rangle_s + |0011\rangle_s)}{4}, \\
 |\chi_{12}\rangle_s &= \frac{1}{2}|0100\rangle_s + \frac{\sqrt{3}}{2}|0001\rangle_s, \\
 |\chi_{21}\rangle_s &= -\frac{1}{2}|1000\rangle_s + \frac{\sqrt{3}}{2}|0010\rangle_s, \\
 |\chi_{03}\rangle_s &= \frac{1}{2}|0010\rangle_s + \frac{\sqrt{3}}{2}|1000\rangle_s, \\
 |\chi_{30}\rangle_s &= \frac{1}{2}|0001\rangle_s - \frac{\sqrt{3}}{2}|0100\rangle_s.
 \end{aligned} \tag{11}$$

The residual term of the output state (7) produced by the most compact five-mode scheme (see Fig. 4) has the form:

$$\begin{aligned}
 |R^{(5,2)}\rangle_{sa} = & \frac{1}{4}\sqrt{\frac{31}{3}}|\chi_0\rangle_s|0\rangle_a + \frac{1}{4}\sqrt{\frac{14}{3}}|\chi_1\rangle_s|1\rangle_a + \\
 & + \frac{1}{4}\sqrt{\frac{2}{3}}|\chi_3\rangle_s|3\rangle_a + \frac{1}{4\sqrt{3}}|0000\rangle_s|4\rangle_a.
 \end{aligned} \tag{12}$$

where

$$\begin{aligned}
 |\chi_0\rangle_s &= \frac{\sqrt{2}}{\sqrt{31}}(|3100\rangle_s - |0130\rangle_s + 2|3001\rangle_s - 2|0031\rangle_s) + \\
 &+ \frac{1}{\sqrt{31}}(|0301\rangle_s - |0400\rangle_s) - \frac{\sqrt{3}}{\sqrt{31}}|1210\rangle_s + \frac{\sqrt{6}}{\sqrt{31}}|1111\rangle_s, \\
 |\chi_1\rangle_s &= \frac{1}{\sqrt{7}}(|3000\rangle_s - |0030\rangle_s) + \\
 &+ \frac{1}{\sqrt{14}}(|0300\rangle_s - \sqrt{3}|0201\rangle_s) - \sqrt{\frac{3}{7}}|1011\rangle_s, \\
 |\chi_3\rangle_s &= \frac{1}{\sqrt{2}}(|0100\rangle_s + |0001\rangle_s).
 \end{aligned} \tag{13}$$

In the scheme with two five-mode interferometers (see Fig. 5), the intermediate state $|\psi'\rangle$, produced by the first interferometer $V_1^{(5)}$ reads:

$$\begin{aligned}
 |\psi'\rangle = & \frac{\sqrt{5}}{3}|\chi'_0\rangle_s|0\rangle_{a1} + \frac{1}{3}\sqrt{\frac{5}{2}}|\chi'_1\rangle_s|1\rangle_{a1} + \\
 & + \frac{1}{3}|\chi'_2\rangle_s|2\rangle_{a1} + \frac{1}{3\sqrt{2}}|0000\rangle_s|3\rangle_{a1},
 \end{aligned} \tag{14}$$

where $|\chi'_j\rangle$ are the following states:

$$\begin{aligned}
 |\chi'_0\rangle_s &= \frac{1}{2}\sqrt{\frac{3}{5}}(|1110\rangle_s + |0111\rangle_s + |0210\rangle_s) + \\
 &+ \frac{1}{\sqrt{10}}(|0021\rangle_s - |1020\rangle_s) + \sqrt{\frac{3}{10}}|1011\rangle_s - \frac{1}{2\sqrt{5}}|0030\rangle_s, \\
 |\chi'_1\rangle_s &= \frac{1}{2}\sqrt{\frac{3}{5}}(|0101\rangle_s + |1100\rangle_s + |0200\rangle_s + |0020\rangle_s) + \\
 &+ \frac{1}{2\sqrt{5}}(|1010\rangle_s - |0011\rangle_s) + \sqrt{\frac{3}{10}}|1001\rangle_s, \\
 |\chi'_2\rangle_s &= \frac{1}{\sqrt{2}}(|0001\rangle_s - |1000\rangle_s).
 \end{aligned} \tag{15}$$

From (14) it follows that single-photon event in mode a1, necessary for heralding, is realized with probability 5/18. Provided that detector D₁ measures one photon at the mode a1, state $|\chi'_1\rangle_s$ enters in the second interferometer $V_2^{(5)}$ that finally produces the state (9) with the residual part

$$\begin{aligned}
 |R^{(5,1,1)}\rangle_{sa} = & 2\sqrt{\frac{2}{11}}|\chi_0\rangle_s|0\rangle_a + 2\sqrt{\frac{2}{11}}|\chi_2\rangle_s|2\rangle_a - \\
 & - \frac{i}{\sqrt{11}}e^{i\alpha}|0000\rangle_s|3\rangle_a
 \end{aligned} \tag{16}$$

where

$$\begin{aligned}
 |\chi_0\rangle_s &= \frac{1}{4} [|2100\rangle + |0120\rangle - i|0300\rangle - i|0003\rangle + \\
 &\quad - e^{i\alpha}(|2001\rangle - |1002\rangle + |0201\rangle - |0021\rangle + |0012\rangle) + \\
 &\quad + e^{-i\alpha}(|1020\rangle - |2010\rangle - |1200\rangle + |0210\rangle + \\
 &\quad + |0102\rangle - i|3000\rangle + i|0030\rangle)], \\
 |\chi_2\rangle_s &= \frac{1}{2} [e^{i\alpha}(|0100\rangle + |1000\rangle - |0010\rangle) + e^{-i\alpha}|0001\rangle].
 \end{aligned}
 \tag{17}$$

and the shorthand $\alpha = \pi/3$ has been introduced to make the expressions more compact.